Article

The Enhanced Oil Recovery Effect of Nitrogen-Assisted Gravity Drainage in Karst Reservoirs with Different Genesis: A Case Study of the Tahe Oilfield

Hong Cheng

No. 2 Oil Production Plant, SINOPEC Northwest Company, Korla 841000, China; chenghong.xbsj@sinopec.com

Abstract: For the Tahe Oilfield, there are multiple sets of karst reservoirs with different genesis developed in carbonate fracture-vuggy reservoirs and the varying karst reservoir type has a considerable influence on the distribution of residual oil. The complex characteristics of different karst reservoirs and the difficulty in producing the remaining oil in the middle and lower part of the reservoir greatly restrict the recovery effects. This work managed to comprehensively investigate the action mechanism of nitrogen-assisted gravity drainage (NAGD) on remaining oil in reservoirs with different karst genesis through modeling and experiments. Based on geological characteristics and modeling results, a reservoir-profile model considering reservoir type, fracture distribution, and the fracture–cave combination was established, the displacement experiments of main reservoirs such as the epikarst zone, underground river, and fault karst were carried out, and the oil–gas–water multiphase flow was visually analyzed. The remaining oil state before and after NAGD was studied, and the difference in recovery enhancement in different genetic karst reservoirs was quantitatively compared. The results show that NAGD was helpful in enhancing oil recovery (EOR) for reservoirs with different karst genesis. NAGD technique has the greatest increasing effect on the sweep efficiency of the fault-karst reservoir, followed by the epikarst zone reservoir, and the smallest in the underground river reservoir. The results of this research will facilitate an understanding of the EOR effect of karst-reservoir types on NAGD and provide theory and technical support for the high-efficiency development in varying karst reservoirs in the Tahe Oilfield.

Keywords: nitrogen-assisted gravity drainage; fracture vuggy; karst reservoirs with different genesis; enhanced oil recovery; carbonate reservoir

1. Introduction

The Tahe Oilfield in Northwest China is mainly a type of carbonate fracture-vuggy reservoir, which is generally characterized by deep burial, large thickness, strong heterogeneity, and multiple sets of reservoirs [1–3]. The karst genesis of the reservoir are various and the reservoir characteristics are complex [4–6]. After natural energy, water flooding, single-well gas injection, and gas flooding in the Tahe Oilfield, oil recovery is still low (18.86%). Although gas flooding has become the main method of enhanced oil recovery (EOR) in the Tahe Oilfield, the EOR is only 1–2%. However, the recovery effect of gas flooding in these reservoirs is not ideal at present and how to enhance oil recovery more effectively through the gas-injection technique is the hot issue in ensuring the stable and effective production of the oilfield. In this regard, experts at home and abroad have begun to attend to and explore nitrogen-assisted gravity drainage (NAGD) techniques [7–12].

Due to multiscale fractures and caves in varying karst reservoirs, lots of remaining oil after water flooding have great development potential; therefore a reasonable and feasible replacement technology needs to be developed urgently [13–15]. The application of the gas-flooding technique shows that the EOR effect of N_2 flooding is significantly different in varying well groups; so, the main action mechanism and core sensitivity factors of gas

flooding to EOR need to be an indepth study. Based on the reservoir characteristics of a fractured-vuggy carbonate oilfield, Lyu et al. [16] established the various visual physical simulation models of the fracture-vuggy combination, which can reflect the real situation of formation, and identified the key influencing factors of gas flooding. The experiment results show that the gas cap formed by injected gas under the action of gravity differentiation could displace the remaining oil which cannot be displaced by injected water on the top of the cave. After water flooding, gas flooding can change the distribution of the pressure and the direction of fluid flow significantly, thus effectively displacing the remaining oil shielded by a high conductive channel. In addition, the gas-flooding stage, like water flooding, is of great significance for reservoir energy replenishment after a large amount of gas is continuously injected into the target reservoir.

The gas-flooding technique in the Tahe Oilfield is effective in enhancing oil recovery after water flooding; however, gas channeling dramatically limits the effect of increased production. Hou et al. [17] established a 2D visual physical model to determine the effects of injection velocity, slug volume, and injection location on the EOR of foam-assisted N_2 technology. The distribution types of remaining oil mainly include loft oil, bypass oil, and oil film. The attic oil at the top of the voids can be replaced by N_2 flooding with a gravity differential. When the injection volume of foam-assisted N_2 reaches a reasonable level, the foam accumulates in the flow passage, reduces the fluid fluidity, and, therefore, effectively inhibits gas channeling, and obviously improves the sweep efficiency of the injection medium. Foam-assisted N_2 has an excellent effect on oil film stripping, oil emulsion, and oil droplet carrying, which improves microdisplacement efficiency [18,19].

A visual fractured-vuggy reservoir model was constructed by Wang et al. [20] on the basis of internal characteristics of the H block in the Xinjiang Oilfield, and a NAGD experiment was carried out. The main influence factor on EOR and remaining oil distribution were studied, including oil-displacement mode, the rate of gas injection, well type of injection and production, and displacement direction. The research results show that, in the NAGD physical simulation experiment process, the range of nitrogen spread and local spread efficiency was determined. The final oil recovery factor of a homogeneous fractured reservoir was higher, the bigger the fracture aperture is, the higher the NAGD recovery factor is. The gas channeling and lower oil recovery can be observed with the greater the amount of gas injection. The gas channeling occurs at the high structural location of the gas-producing outlet; therefore, the gas channeling should be controlled and plugged in time to improve the utilization ratio of injected gas [21–24].

The main types of reservoir space structures are large-scale karst cavities and fractures, with different sizes, irregular shapes, and discontinuous distribution in the Tahe Oilfield. Quantitative characterization of the distribution of pores, cavities, and fractures in the 3D physical simulation models has always been a technical problem due to its complexity and restricting the efficient development of serious heterogeneous reservoirs. Hu et al. [25] have developed a 3D geological modeling method with multiple constraints aimed at the Tahe Oilfield. First, a discrete karst cave and fracture model were established using seismic identification data and deterministic modeling methods. Under the constraint of karst phase control, the multiattribute cooperative simulation method of stochastic modeling was adopted to establish the karst cavity model and discrete small-scale fracture model. Finally, four single-type models were fused into a multiscale discrete fracture-cave reservoir 3D geological model by using the collocation condition assignment algorithm.

It is of great significance to explore and investigate the core action mechanism of the typical fracture propagation and to consider the effect of the karst cave on fracture propagation for optimizing the fracturing scheme and improving the probability of fracture-cave connection in a carbonate reservoir. To deeply study the fracture development law of the carbonate reservoir, Guo et al. [26] combined with the damage mechanics theory and carried out the numerical simulation through the seepage–stress–damage coupling equation; the accuracy of the numerical simulation was verified by the experimental results. The results show that there are four types of crack propagation, including block, direct span,

cross after deflection, and deflection. In addition, the pressure curve can be subdivided into the initial initiation, pressure release stages in the karst cave, pressure region in the karst cave, refracture, and fracture propagation zones. The difference in horizontal principal stress is the principal influence factor that affects the growth trend of fractures and the occurrence of branch fractures.

Accurate determination of the distribution characteristics of fractures, cavities, and the remaining oil has become one of the major constraints to stable and enhanced production in the Tahe Oilfield. Du et al. [27] used microgravity monitoring technology to achieve an accurate characterization of fracture–cavity distribution. The lower part of the fracture-cave structure in the target block was connected with the middle part, while the southern part of the fracture–cave system was significantly connected with the middle part, resulting in different development effects in N_2 flooding. The research results provide significant technique guidance for adjusting and setting the reasonable injection-production scheme and improving the EOR effect.

Based on the research data of fault-controlled palaeokarst in Tahe Oilfield, Zhang et al. [28,29] proposed a layered modeling method for palaeokarst combined with the theory of principles of layered constraint and genetic control. Fault-controlled palaeokarst can be divided into strike-slip fault impact zone, fault-controlled outer palaeokarst enclave, fault-controlled inner palaeokarst structure, and karst-cave filling. The karst pore and the discrete small-scale fracture distribution models were obtained by sequential indicator simulation and target-based punctuation process simulation. The validation results in the TP area of Tahe Oilfield show that the 3D integrated model could reflect the spatial levels of palaeokarst carbonate reservoirs controlled by faults.

The comprehensive review of the above-mentioned research shows that there are three typical reservoirs in fractured-vuggy carbonate reservoirs according to different karst genesis, which are epikarst zone, underground river, and fault-karst reservoirs, the type of karst reservoir formed by different factors has an important effect on the distribution of remaining oil, especially on EOR effects under varying oil recovery methods. In these works, the model was made according to the distribution probability of fractures and caves in the reservoir, not based on the geological model. And there is a certain gap between its structure and the actual reservoir; therefore, the results of the study cannot directly reflect the actual situation in the oilfield.

In this work, physical models of karst reservoirs of different karst genesis based on geological models were established. The experiments of natural bottom water flooding, artificial water flooding, and N_2 flooding were carried out to obtain the distribution characteristics of the remaining oil in the various karst reservoirs. Then, the NAGD experiment was carried out. The research results are in favor of understanding the feasibility of NAGD and the effect of different reservoir types on quantitative productivity analysis and providing theoretical and technical support for the development of fracture-vuggy reservoirs in the Tahe Oilfield.

2. Visual Karst-Reservoir Model

The accurate identification and description of the fracture-cave reservoir, especially the spatial distribution of the fracture-cave and the relationship between the well-cave and well-fracture are the basis of making a reasonable development scheme. Based on the geophysics method, the spatial structure representation technique of fracture-cavity is used to characterize the fracture-cavity body. By further clearing up the spatial relations of varying reservoirs, including fracture-cave, cave-cave, and well-cave, a comprehensive description of actual reservoirs with different scales and types can be realized.

For the karst reservoir of different genesis, including the epikarst zone reservoir, underground river reservoir, and fault-karst reservoir, the basic design and manufacturing process of the 2D visual physical profile model is as follows. First, construct the geological model of the reservoir structural area based on numerical simulation technology. Second,

the physical model of a 2D section used in oil-displacement experiments is established and the visual physical model is formed by physical etching.

The method of deterministic modeling and stochastic modeling established in the 1980s has solved the problem of geostatistical modeling of continuous porous reservoirs. The method of multipoint geostatistics and discrete fracture modeling established at the beginning of the 21st century has solved the geological modeling problem of river channels and fractured reservoirs. The discrete fracture-vuggy modeling method for fractured-vuggy reservoirs solves the problem of geologic modeling for karst composite reservoirs. Controlled and influenced by multistage tectonic movement and other factors, the palaeokarst reservoir is the most important reservoir type in uplift. The discrete fracture-cavity modeling technique divides the karst reservoir into karst cave, fracture (large scale, mesoscale, and small scale), and bedrock. Under the constraints of palaeogeomorphology, karst-reservoir development model, and fracture-development law, the discrete distribution model is established by classification and then fused to form a 3D geological model of a discrete karst cave-fracture network.

The first step is to construct the 3D geological model of the study area by Petrel E&P Platform software based on the geological structure information. Combined with the geological characteristics and main parameters of the TK667-TK666-TK602 well group in the Tahe Oilfield, a geological model of the reservoir in the epikarst zone was established. As shown in Figure 1, typical structures in the model, such as cracks and caves, are marked, with the regions of cracks in green and caves in yellow. The second step is to analyze the well-group structure by observing the geological model and cutting the geological model vertically by designing the section of connecting wells. The third step is to delineate the development and distribution area according to the fracture morphology (opening, length, and strike) and the cave characteristics (height, length, thickness, etc.). The fourth step is to use seismic and body data to restore the medium- and small-scale fractures in the 2D section and, then, according to the size of the geological model to scale, to obtain a 2D section model of 300 mm × 600 mm in size, as shown in Figure 2. In the fifth step, the final section physical model is etched on the plexiglass plate based on the above fracture-cavity model distribution map. As shown in Figure 3, the 2D visual physical profile models of the epikarst zone, underground river, and fault-karst reservoirs can be obtained respectively according to the above steps.
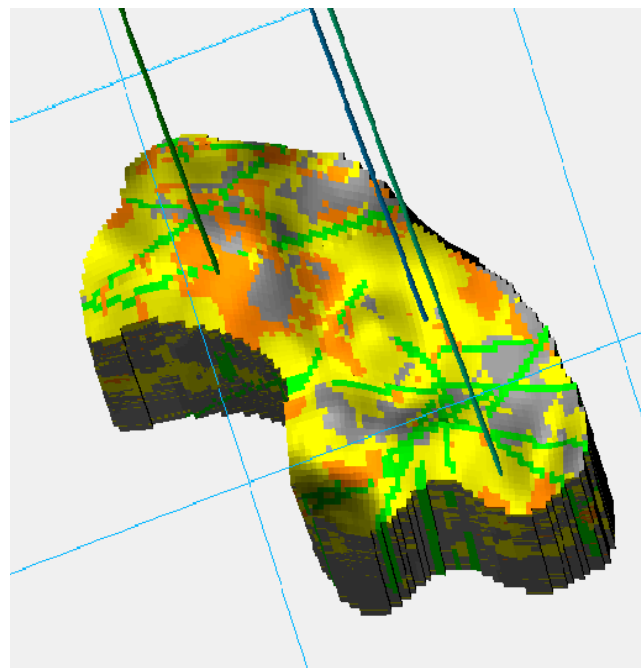

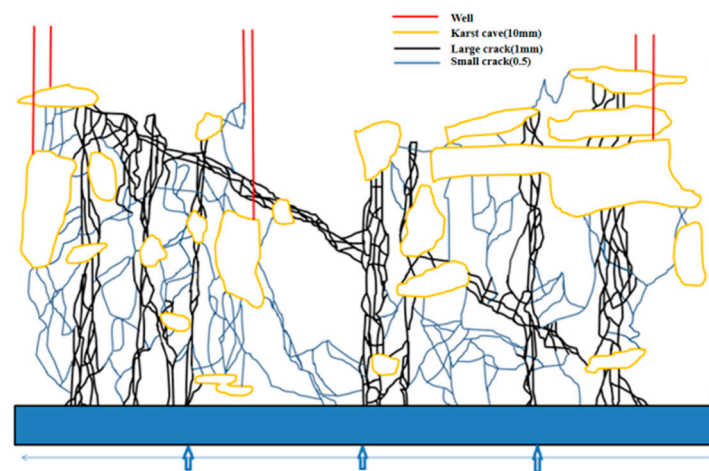**Figure 1.** The 3D profile model of the target well group constructed in Petrel software.

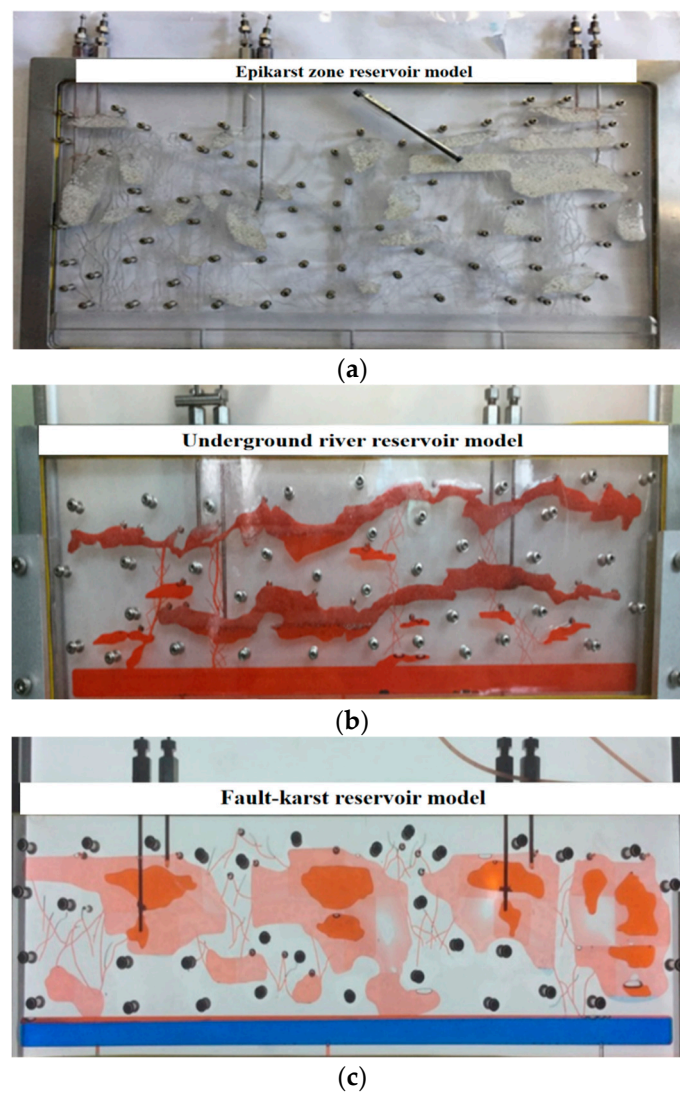**Figure 2.** Design of fracture and cave distribution in the epikarst zone reservoir.

Figure 3. Visual experimental models of different genetic reservoirs. (**a**) Epikarst zone reservoir model; (**b**) Underground river reservoir model; (**c**) Fault-karst reservoir model.

In this work, the model of the karst reservoir is made of an acrylic plate. To ensure the wettability of the model material, the model material was immersed in water before the physical model experiment. It is found that water droplets with a fixed wetting angle

(about 62°) are formed on the surface of model materials of the karst reservoir. The results show that the wettability of model materials of the karst reservoir is similar to that of the actual reservoir.

3. Experimental Section

3.1. Apparatus

According to the similarity criterion, the parameters and conditions of the visual physical model of a 2D fractured-vuggy karst reservoir are determined to ensure that the model accords with the actual situation. Fluid channels in fractured-vuggy reservoirs are complex and varied, and flow patterns are not unique. Therefore, we cannot satisfy many similarity criteria in the same model; so, we can only simulate some fluids with similarity and focus on geometric similarity, motion similarity, and dynamic similarity design of the karst reservoir. In addition, because the fluid flow in the reservoir is mainly affected by gravity differentiation, dynamic similarity design, gravity, and formation pressure are mainly considered and the effect of viscous force is ignored.

Based on the visualized physical experimental models of karst-reservoir types of different genesis, the oil-displacement experiments of the 2D visual physical model of natural bottom water flooding, artificial water flooding, N_2 flooding, and nitrogen-assisted gravity drainage were carried out successively to simulate the actual field and the remaining oil occurrence state of the karst reservoir with different genesis in the development stage is studied.

As shown in Figure 4, the physical simulation experimental apparatus is mainly connected with a physical model with a slot, a fluid injection, a receiving and metering device, a displacement pump, and a piston-type intermediate vessel for holding simulated crude oil and formation water. The upper pressure limit of the displacement pump is 30 MPa and the range of flow rate is between 0.01 and 10 mL/min. The maximum capacity of the piston-type intermediate vessel is 1 L, and the working pressure is between 0 and 32 MPa. With this device, the experiments of saturated oil, bottom water flooding, gas flooding, and nitrogen-assisted gravity drainage can be carried out on the fracture-cavity physical model. The oil–water metering and pressure detection system is composed of a measuring cylinder and a pressure-difference sensor connected to a computer. The experimental process and phenomena are recorded by a Logitech Pro C922 camera with a resolution of 800×320 pixels.

1) **Gas Flow Controllers;**
2) **Pressure measuring devices;**
3) **Experimental photography set-up;**
4) **Oil, gas and water metering devices;**
5) **Fault-karst model;**
6) **Simulation oil devices;**
7) **Simulation of water injection devices;**
8) **Simulation of bottom water devices;**
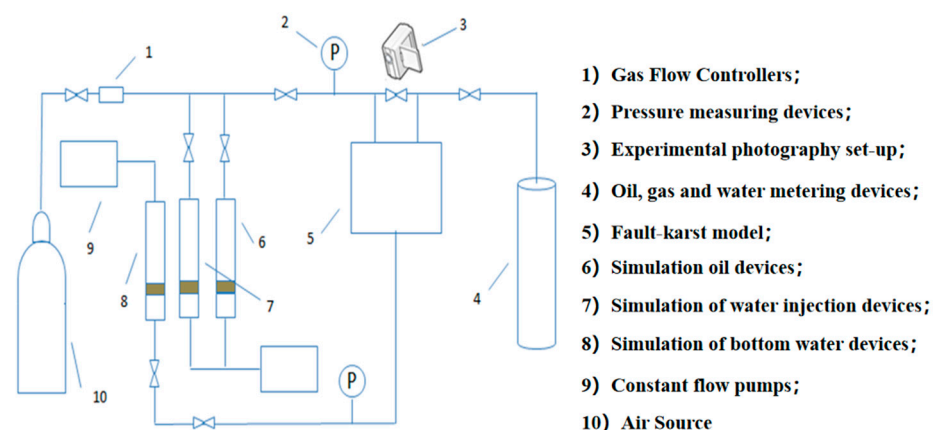9) **Constant flow pumps;**
10) **Air Source**

Figure 4. Simplified schematic of the oil-displacement experimental setup under the varying visual physical model.

The oil-displacement experimental temperature is 25 °C and the pressure is normal. First, the aviation kerosene and paraffin oil were mixed in a certain proportion to simulate the formation fluid configuration, and the viscosity was about 23.8 mPa·s. Secondly, the simulated formation water had a density of 1.032 g/m and salinity of 220 g/L [30]. The oil-displacement experiment was carried out with high-pressure N_2 with a viscosity of

0.0178 mPa·s [31]. In addition, methyl blue tone is blue in the simulated formation water and Sudan red tone is red in the simulated oil, so that the distribution of oil–water in two phases can be observed.

3.2. Oil-Displacement Experimental Scheme

The three karst-reservoir physical models and the experimental device are used to carry out the operation of the saturated simulated oil through the bottom entrance of the physical model and record the saturated simulated oil quantity. Then, fill the bottom water tank with simulated formation water and record. The total volume of fracture-cavity media is the amount of saturated oil minus the amount of saturated formation water. Then, three typical karst-reservoir physical models of different genesis are simulated by natural bottom water flooding, artificial water flooding, N_2 flooding, and NAGD. Finally, the final state of the remaining oil from three typical reservoir types is obtained and their effects on enhanced oil recovery are compared and analyzed.

(a)   Natural bottom water flooding

The simulated formation water is injected through the bottom water inlet to record the water cut and the change of the injected simulated formation water pressure. When the water cut of any well outlet reaches 98%, the outlet of the well is closed, and the natural bottom water flooding of the well ends.

(b)   Artificial water flooding

With this well, as an injection well, the other wells are produced and the water cut changes of the produced wells with a water cut of less than 98% are recorded in real time; when the final water cut of the produced wells is more than 98%, the corresponding produced wells are closed.

(c) N_2 flooding

The N_2 is injected into the water injection wells that have completed the water flooding, the bottom water inlet is opened, and the other wells are produced. When gas channeling occurs, the well is closed and the gas-flooding experiment is finished.

(d)   Nitrogen-assisted gravity drainage (NAGD)

After the completion of N_2 flooding with a low injection and high production, the high recovery wells are treated as N_2 injection wells, the low recovery wells are treated as recovery wells, and the relationship between water cut, gas-oil ratio, and injection pressure of the injection well with injection volume is recorded in real time. When gas channeling occurs, the production well is closed and the experiment in nitrogen-assisted gravity drainage is finished.

4. Distribution Characteristics of Remaining Oil in Different Karst Reservoirs and Influencing Factors

By changing the factors such as cavity filling, fracture development, water multiple, and injection-production height difference in the carbonate reservoir, the displacement experiments of 2D profile models of the epikarst zone, underground river, and fault-karst reservoirs were carried out. This paper mainly includes the simulation experiments of nitrogen-assisted gravity drainage after natural water flooding, artificial water flooding, and N_2 flooding, and analyzes the characteristics and influencing factors of NAGD in different reservoir types.

4.1. Epikarst Zone Reservoir

The topmost epikarst zone is a very important part of each karst zone and it is a window to further explore the development law of the fracture-cavity karst reservoir, as shown in Figure 5. Under different karst geomorphology conditions, the karstification mode and intensity are different, which leads to the different development thickness of the epikarst zone in different karst geomorphology locations. The development thickness of

the epikarst zone is closely related to lithology, palaeogeomorphology, geological structure, palaeoclimate, hydrodynamic condition, and development of the palaeosoil layer. The epikarst zone in the Tahe oilfield is mainly developed by the surface river, water hole, slope deposit, and ordovician limestone, and is accompanied by fractures and faults.
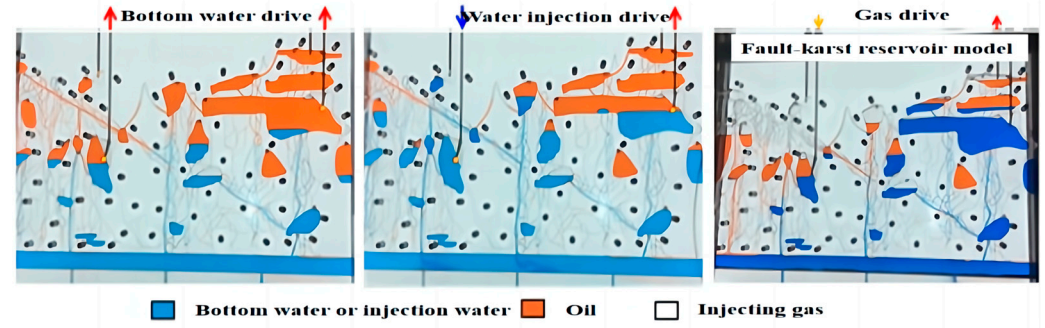

Figure 5. Experimental diagram of 2D section model at varying displacement stages in epikarst zone reservoir.

In the natural water drive stage, the simulated oil in the lower part of the physical model of the reservoir in the epikarst zone is mainly displaced. After bottom water flooding, the enrichment of remaining oil in the upper part of the oil–water interface and blind-end hole can be observed obviously. After artificial water flooding, the remaining oil between wells is further displaced to production wells and then transferred to gas flooding (low injection and high production). According to the distribution of the remaining oil, the injected gas moves up to the highest point of the reservoir, and then transversely to the bottom of the production well. The enrichment of the remaining oil between the wells and the lower part of the production horizon can be observed during gas flooding.

After nitrogen-assisted gravity drainage (high injection and low production), the oil–gas–water three-phase distribution of the displacement experiment is shown in Figure 6. There are three main types of injection-gas flooding to replace remaining oil in the gas-flooding epikarst zone reservoir model stage. First, the injected gas can effectively displace the remaining oil around the gas injection well. Second, with the continuous increase of injected gas, lateral migration of injected gas can displace the remaining oil around the produced well. Third, the injected gas accumulates in the upper space of the reservoir and displaces the remaining oil between wells in the reservoir downwards.
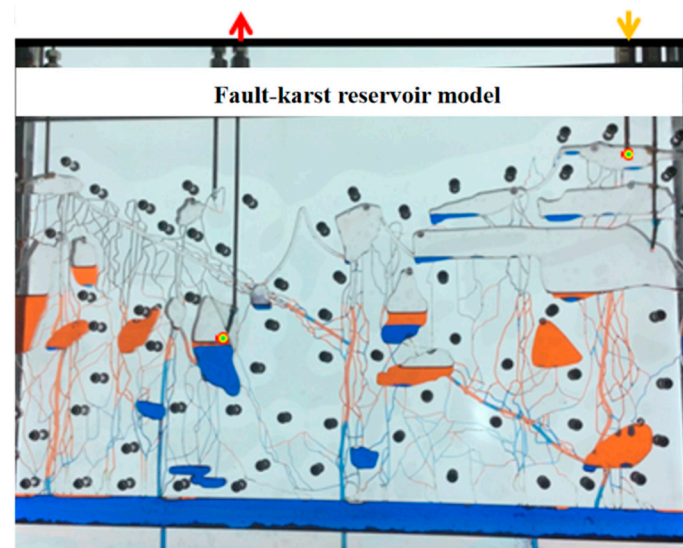

Figure 6. Nitrogen-assisted gravity drainage (high injection and low production).

The results of the nitrogen-assisted gravity-drainage experiment in the epikarst zone reservoir physical model are shown in Figure 7. Compared with N_2 flooding, the NAGD stage can fully play the role of gravity. Therefore, in the NAGD stage, it is easier to realize uniform displacement and greatly improve sweep efficiency to effectively enhance the degree of remaining oil recovery in the reservoir. For the epikarst zone reservoir, NAGD flooding can improve the recovery by 8.85% compared with low injection-high production N_2 flooding.
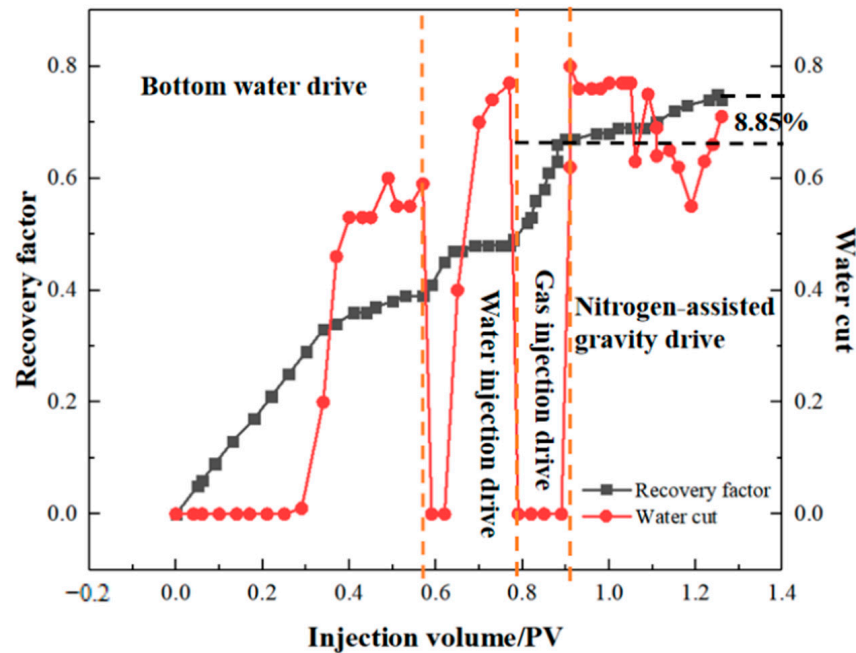

Figure 7. Oil recovery factor and water cut in different displacement stages in epikarst zone reservoir.

4.2. Underground River Reservoir

The underground river karst reservoir of the carbonate reservoir is composed of a deep main underground river, shallow underground river, and high-angle fracture. The reservoir space is composed of caves, holes, and fractures, and the distribution of the underground river is continuous on the whole. In addition, the high-angle fractures developed locally, which connected the upper and lower layers of the underground river and formed a whole set of underground river–karst systems.

The nitrogen-assisted gravity-drainage experiments were carried out on the underground river reservoir model after natural bottom water flooding, artificial water flooding, and N_2 flooding. The remaining oil from natural water flooding and artificial water flooding is mainly the remaining oil around the production well. N_2 flooding with a low injection rate and high production rate mainly displaces the remaining oil in the upper part of the connecting path and can enlarge the extent and volume of water to the remaining oil. In the NAGD experiment with a high injection rate and low recovery rate, the injected gas can be further injected into the upper space and accumulate to displace the remaining oil between wells that have not been displaced in the earlier development process, further enhancing oil recovery. The distribution characteristics of remaining oil after different displacement stages in the underground river reservoir physical model are shown in Figure 8. The NAGD method is more effective than other recovery methods in displacing the remaining oil in the underground river reservoir and can effectively restrain the water coming to a height at the bottom of the injection well, thus improving the oil recovery factor.
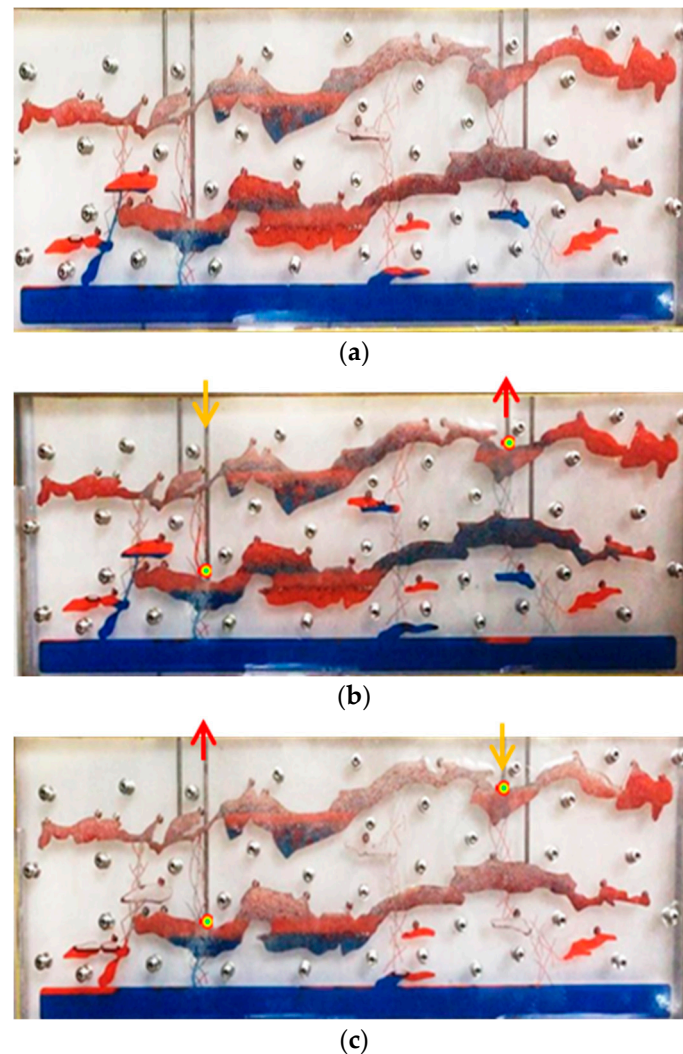
(a)

(b)

(c)

Figure 8. Residual oil-distribution map of underground river reservoir at various displacement stages. (**a**) End of water flooding; (**b**) End N_2 flooding, low injection, and high production; (**c**) End nitrogen-assisted gravity drainage, high injection, and low production.

The experimental results of nitrogen-assisted gravity drainage at varying displacement stages in the underground river reservoir are shown in Figure 9. The NAGD technique can effectively start the interwell residual oil in underground river reservoirs and the final oil recovery factor is lower than that of N_2 flooding of low injection and high injection by 6.28%.

It can be seen that in the bottom water flooding stage, the recovery degree increases significantly before the injection amount of 0.5 PV. In the stage of artificial water flooding, the recovery degree decreases first and then recovers quickly. The gas flooding with a low injection rate and the high recovery rate was carried out after two water floodings. Since the water-flooding to gas-flooding switch is not smooth during the experiment, the gas-flooding in the initial stage of the recovery degree dropped sharply, rose rapidly in a short time, and then changed a little over a long time.

4.3. Fault-Karst Reservoir

The fault-karst trap, as a new type and target of oil and gas recovery in deep marine carbonate rocks, has been widely recognized by the industry and widely applied in the Tarim Basin. Compared with the traditional fracture-pore carbonate traps and the typical Kras reservoir at home and abroad, the fault-karst trap in the Tahe Tarim Basin is characterized by deep burial, strong reservoir heterogeneity, and great difference in fluid properties.

It is difficult to form, classify, and characterize fault-karst traps, so we cannot use the existing reservoir geological models, trap classification, and characterization methods at home and abroad for reference.
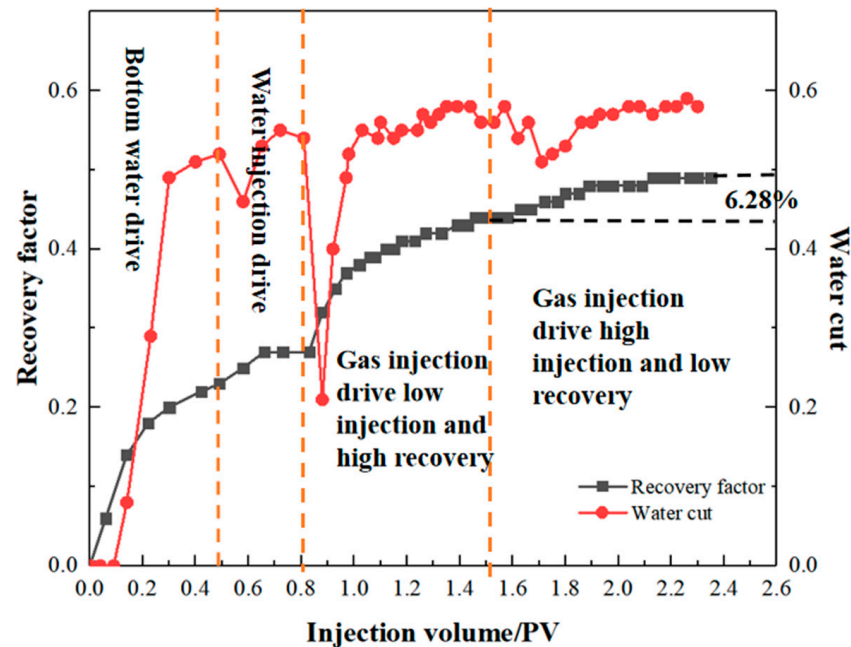

Figure 9. Oil recovery factor and water cut in different displacement stages of underground river reservoirs.

The distribution characteristics of the remaining oil in varying displacement stages in the fault-karst reservoir are shown in Figure 10. In the carbonate reservoirs of the Tahe Oilfield, the distribution of karst caves in the fault-karst reservoir is relatively wide compared with that in the epikarst zone and the underground river reservoirs. Natural bottom water flooding, artificial water flooding, N_2 flooding, and NAGD were in turn carried out on the physical model of the fault-karst reservoir.

The natural bottom water flooding method mainly displaces the remaining oil in the downhole along the reservoir passage system and it is easy to generate water coming to seal the remaining oil between wells. The injected water of artificial water flooding easily forms high pressure around the injection well; thus, a large pressure difference is formed between the injection and the production wells. Rapid water channeling easily occurs and the lateral displacement efficiency is low. The injection gas tends to gather at the top of the production well, the injection fluid is mainly longitudinal flow, the transversal displacement is less, and the production well is in a low-pressure area. Therefore, gas channeling occurs easily. Thus, it is difficult to extract the remaining oil around the injection well and between well groups. The injection gas of NAGD can accumulate in the high part of the reservoir and can displace oil between wells, effectively displacing the remaining oil which is sealed in the reservoir. It is characterized by "initial inhibition of bottom water and overall gas-water synergy". The physical simulation experimental results of different displacement stages are shown in Figure 11. Nitrogen-assisted gravity drainage can increase recovery by 11.7% compared with the gas flooding of low injection and high production.

4.4. Comparison of EOR Effect

The contrast results of the degree of enhanced oil recovery by nitrogen-assisted gravity drainage on varying karst reservoirs are shown in Figure 12. The enhanced oil recovery of NSGD to the epikarst zone, underground river, and fault-karst reservoir are 8.85%, 6.28%, and 11.70%, respectively. Compared with the epikarst zone and fault-karst, NAGD technology has no obvious recovery effect on underground river reservoirs. It is believed that the

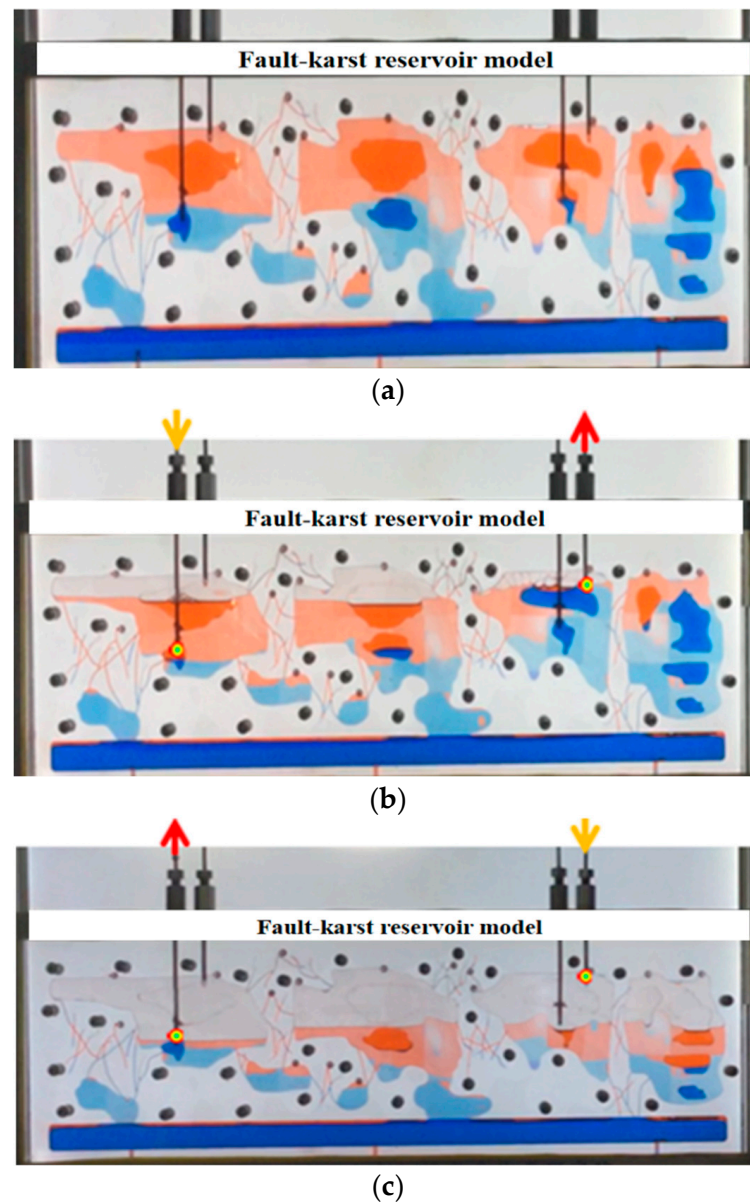phenomenon is related to the unique and complex characteristics of the underground river reservoir.

Figure 10. Residual oil-distribution map of fault-karst reservoir at various displacement stages. (**a**) End of water flooding; (**b**) End N_2 flooding, low injection, and high production; (**c**) End nitrogen-assisted gravity drainage, high injection, and low production.

The study shows that the underground river is a karst cave and underground passage formed by karstification in a large area of limestone, and its development and shape are often controlled by geological structure and fissures. According to the morphological characteristics of the underground river reservoir, can be divided into branches, serrated, linear, net-like, and so on.

On the whole, the NAGD method is helpful to realize balanced displacement and improve recovery degree for reservoirs with different karst genesis. The enhanced recovery of nitrogen-assisted gravity flooding is the best in fault-solution reservoirs, the second in epikarst zone reservoirs, and the least in underground river reservoirs.
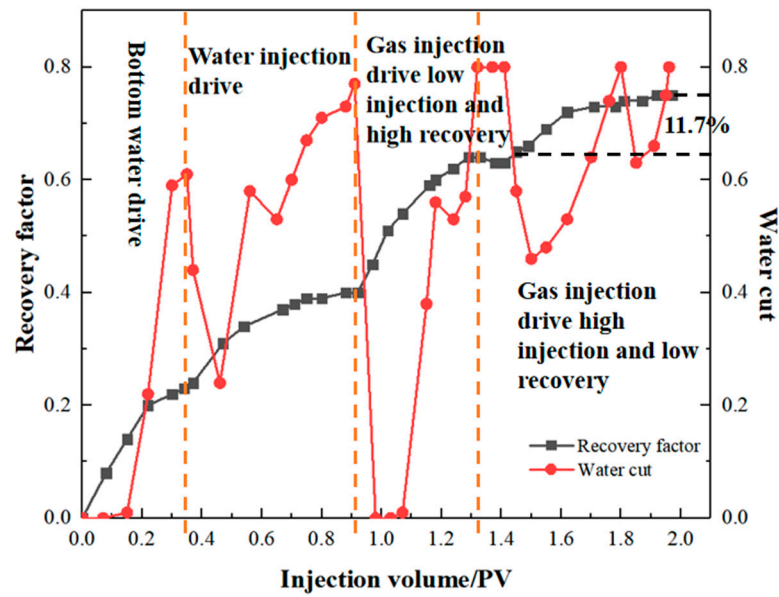
Figure 11. Oil recovery factor and water cut in different displacement stages of fault-karst reservoir.
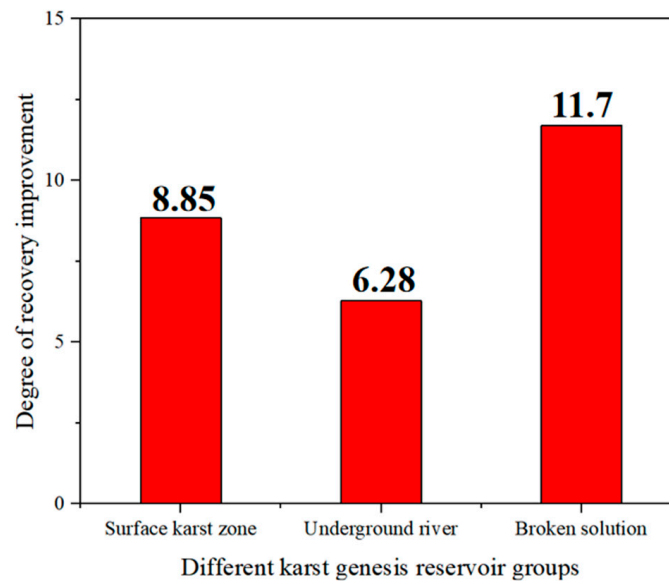

Figure 12. Comparison of enhanced oil recovery effects by nitrogen-assisted gravity drainage in karst reservoirs with different genesis.

5. Conclusions

Combined with geological feature and modeling results, a reservoir profile model considering reservoir type, fracture distribution, and fracture–fracture–cavity combination was established, the displacement experiments of main reservoirs such as the epikarst zone, underground river, and fault-karst reservoirs were carried out, and the oil–gas–water multiphase flow was visualized. The remaining oil state before and after nitrogen-assisted gravity drainage was studied, and the difference in recovery enhancement degree in different genetic karst reservoirs was quantitatively compared. The main conclusions are described below.

(1) For the epikarst zone reservoir, it is easier to realize uniform displacement and greatly improve sweep efficiency in the NAGD stage to effectively enhance the degree of remaining oil recovery in the reservoir. NAGD flooding can improve the recovery by 8.85% compared with low injection-high production N_2 flooding;

(2) For the underground river reservoirs, NAGD flooding can effectively start the inter-well residual oil in underground river reservoirs and the final oil recovery factor is lower than that of N_2 flooding of low-injection and high-injection by 6.28%;

(3) The injection gas tends to gather at the top of the production well, the injection fluid is mainly longitudinal flow, the transversal displacement is less, and the production well is in a low-pressure area; therefore, gas channeling occurs easily. For the fault-karst reservoir, the NAGD technique could increase recovery by 11.7% compared with gas flooding of low injection and high production.

The experiment result shows that nitrogen-assisted gravity drainage technology can enhance the recovery of fault-karst reservoirs to the greatest.

Conflicts of Interest: The author declares that he has no known competing financial interests or personal relationships that could have appeared to influence the work reported in this paper.

References

1. Ma, X.; Li, H.; Luo, H.; Nie, S.; Gao, S.; Zhang, Q.; Yuan, F.; Ai, W. Research on well selection method for high-pressure water injection in fractured-vuggy carbonate reservoirs in Tahe oilfield. *J. Pet. Sci. Eng.* **2022**, *214*, 110477. [CrossRef]
2. Kouassi, A.K.F.; Pan, L.; Wang, X.; Wang, Z.; Mulashani, A.K.; James, F.; Nyakilla, E.E. Identification of karst cavities from 2D seismic wave impedance images based on Gradient-Boosting Decision Trees Algorithms (GBDT): Case of ordovician fracture-vuggy carbonate reservoir, Tahe Oilfield, Tarim Basin, China. *Energies* **2023**, *16*, 643.
3. Sheng, S.; Duan, Y.; Wei, M.; Yue, T.; Wu, Z.; Tan, L. Analysis of interwell connectivity of tracer monitoring in carbonate frac-ture-vuggy reservoir: Taking T-well group of Tahe Oilfield as an example. *Geofluids* **2021**, *2021*, 5572902. [CrossRef]
4. Geng, F.; Li, B.; Yang, S.; Hu, B.; Zheng, J. Study on probabilistic distribution model of reserves calculation coefficient in the fractured-vuggy reservoir of Tahe Oilfield, Tarim Basin, China. *Environ. Earth Sci.* **2022**, *81*, 135. [CrossRef]
5. Song, Z.J.; Li, M.; Zhao, C.; Yang, Y.L.; Hou, J.R. Gas injection for enhanced oil recovery in two-dimensional geology-based physical model of Tahe fractured-vuggy carbonate reservoirs: Karst fault system. *Pet. Sci.* **2020**, *17*, 419–433. [CrossRef]
6. Zhang, T.; Zeng, X.; Guo, J.; Zeng, F.; Li, M. Numerical simulation on oil-water-particle flows in complex fractures of fractured-vuggy carbonate reservoirs. *J. Pet. Sci. Eng.* **2022**, *208*, 109413. [CrossRef]
7. Salifou, I.A.M.; Zhang, H.; Boukari, I.O.; Harouna, M.; Cai, Z. New vuggy porosity models-based interpretation methodology for reliable pore system characterization, Ordovician carbonate reservoirs in Tahe Oilfield, North Tarim Basin. *J. Pet. Sci. Eng.* **2021**, *196*, 107700. [CrossRef]
8. Qu, M.; Hou, J.; Wen, Y.; Liang, T. Nitrogen gas channeling characteristics in fracture-vuggy carbonate reservoirs. *J. Pet. Sci. Eng.* **2020**, *186*, 106723. [CrossRef]
9. Yue, P.; Xie, Z.; Liu, H.; Chen, X.; Guo, Z. Application of water injection curves for the dynamic analysis of fractured-vuggy carbonate reservoirs. *J. Pet. Sci. Eng.* **2018**, *169*, 220–229. [CrossRef]
10. Yang, B.; He, J.; Lyu, D.; Tang, H.; Zhang, J.; Li, X.; Zhao, J. Production optimization for water flooding in fractured-vuggy carbonate reservoir—From laboratory physical model to reservoir operation. *J. Pet. Sci. Eng.* **2020**, *184*, 106520. [CrossRef]
11. Yue, P.; Xie, Z.; Huang, S.; Liu, H.; Liang, S.; Chen, X. The application of N_2 huff and puff for IOR in fracture-vuggy carbonate reservoir. *Fuel* **2018**, *234*, 1507–1517. [CrossRef]
12. Wang, Y.; Hou, J.; Tang, Y.; Song, Z. Effect of vug filling on oil-displacement efficiency in carbonate fractured-vuggy reservoir by natural bottom-water drive: A conceptual model experiment. *J. Pet. Sci. Eng.* **2019**, *174*, 1113–1126. [CrossRef]
13. Zheng, S.; Yang, M.; Kang, Z.; Liu, Z.; Long, X.; Liu, K.; Zhang, S. Controlling factors of remaining oil distribution after water flooding and enhanced oil recovery methods for fracture-cavity carbonate reservoirs in Tahe Oilfield. *Pet. Explor. Dev.* **2019**, *46*, 786–795. [CrossRef]
14. Li, K.; Chen, B.; Pu, W.; Wang, J.; Liu, Y.; Varfolomeev, M.; Yuan, C. Numerical simulation via CFD methods of nitrogen flooding in carbonate fractured-vuggy reservoirs. *Energies* **2021**, *14*, 7554. [CrossRef]
15. Wang, J.; Qi, X.; Liu, H.; Yang, M.; Li, X.; Liu, H.; Zhang, T. Mechanisms of remaining oil formation by water flooding and enhanced oil recovery by reversing water injection in fractured-vuggy reservoirs. *Pet. Explor. Dev.* **2022**, *49*, 1110–1125. [CrossRef]
16. Lyu, X.; Liu, Z.; Hou, J.; Lyu, T. Mechanism and influencing factors of EOR by N_2 injection in fractured-vuggy carbonate reservoirs. *J. Nat. Gas Sci. Eng.* **2017**, *40*, 226–235. [CrossRef]
17. Hou, J.; Luo, M.; Zhu, D. Foam-EOR method in fractured-vuggy carbonate reservoirs: Mechanism analysis and injection pa-rameter study. *J. Pet. Sci. Eng.* **2018**, *164*, 546–558. [CrossRef]
18. Liang, L.; Hou, J. Fluids flow behaviors of nitrogen and foam-assisted nitrogen floods in 2D visual fault-karst carbonate reservoir physical models. *J. Pet. Sci. Eng.* **2021**, *200*, 108286. [CrossRef]

19. Qu, M.; Liang, T.; Hou, J. Study on fluid behaviors of foam-assisted nitrogen flooding on a three-dimensional visualized frac-ture-vuggy model. *Appl. Sci.* **2021**, *11*, 11082. [CrossRef]

20. Wang, J.; Ji, Z.; Liu, H.; Huang, Y.; Wang, Y.; Pu, Y. Experiments on nitrogen assisted gravity drainage in fractured-vuggy reservoirs. *Pet. Explor. Dev.* **2019**, *46*, 355–366. [CrossRef]

21. Wang, T.; Wang, L.; Qin, H.; Zhao, C.; Bai, Z.; Meng, X. Identification of gas channeling and construction of a gel-enhanced foam plug-ging system for oxygen-reduced air flooding in the Changqing Oilfield. *Gels* **2022**, *8*, 373. [CrossRef] [PubMed]

22. Wang, C.; Ma, B.; Zhang, L. Experimental study on CO_2 capture by using n-butylamine to plug the gas channeling to enhanced oil recovery. *J. Pet. Explor. Prod. Technol.* **2022**, *12*, 2523–2531. [CrossRef]

23. Luo, X.-J.; Wei, B.; Gao, K.; Jing, B.; Huang, B.; Guo, P.; Yin, H.-Y.; Feng, Y.-J.; Zhang, X. Gas channeling control with an in-situ smart surfactant gel during water-alternating-CO_2 enhanced oil recovery. *Pet. Sci.* **2023**. [CrossRef]

24. Dong, S.; Li, L.; Wu, Y.; Huang, X.; Wang, X. Preparation and Study of Polyvinyl Alcohol Gel Structures with Acrylamide and 2-Acrylamido-2-methyl-1-propanesulfonic Acid for Application in Saline Oil Reservoirs for Profile Modification. *ACS Appl. Mater. Interfaces* **2023**, *15*, 14788–14799. [CrossRef]

25. Hou, J.R.; Zheng, Z.Y.; Song, Z.J.; Luo, M.; Li, H.B.; Zhang, L.; Yuan, D.Y. Three-dimensional geological modeling of fractured-vuggy carbonate reservoirs: A case from the Ordovician reservoirs in Tahe-IV block, Tahe oilfield. *Oil Gas Geol.* **2013**, *34*, 383–387.

26. Guo, T.; Tang, S.; Li, Y.; Zhou, F.; Tan, B.; Qu, Z.; Ling, K. The Effect of dissolved cavern on the fracture propagation in vuggy carbonate reservoir. *J. Energy Resour. Technol.* **2021**, *143*, 053003. [CrossRef]

27. Du, C.; Yin, C.; Cheng, H.; Yuan, F.; Zhao, Y. Microgravity Monitoring in Fractured-Vuggy Carbonate Reservoirs. *Geofluids* **2023**, *2023*, 5034948. [CrossRef]

28. Zhang, W.; Duan, T.; Li, M.; Zhao, H.; Shang, X.; Wang, Y. Architecture characterization of Ordovician fault-controlled paleokarst carbonate reservoirs in Tuoputai, Tahe oilfield, Tarim Basin, NW China. *Pet. Explor. Dev.* **2021**, *48*, 367–380. [CrossRef]

29. Zhang, W.; He, Z.; Duan, T.; Li, M.; Zhao, H. Hierarchical modeling of carbonate fault-controlled paleokarst systems: A case study of the ordovician reservoir in the Tahe Oilfield, Tarim Basin. *Front. Earth Sci.* **2022**, *10*, 840661. [CrossRef]

30. Li, Y.; Kang, Z.; Xue, Z.; Zheng, S. Theories and practices of carbonate reservoirs development in China. *Pet. Explor. Dev.* **2018**, *45*, 712–722. [CrossRef]

31. Du, X.; Li, Q.; Lu, Z.; Li, P.; Xian, Y.; Xu, Y.; Li, D.; Lu, D. Pressure transient analysis for multi-vug composite fractured vuggy carbonate reservoirs. *J. Pet. Sci. Eng.* **2020**, *193*, 107389. [CrossRef]